

Macromolecular Fingerprinting of *Sulfolobus* Species in Biofilm: A Transcriptomic and Proteomic Approach Combined with Spectroscopic Analysis

Andrea Koerdt,^{†,‡} Alvaro Orell,^{†,‡} Trong Khoa Pham,[§] Joy Mukherjee,[§] Alexander Wlodkowski,[†] Esther Karunakaran,[§] Catherine A. Biggs,[§] Phillip C. Wright,[§] and Sonja-Verena Albers^{*,†}

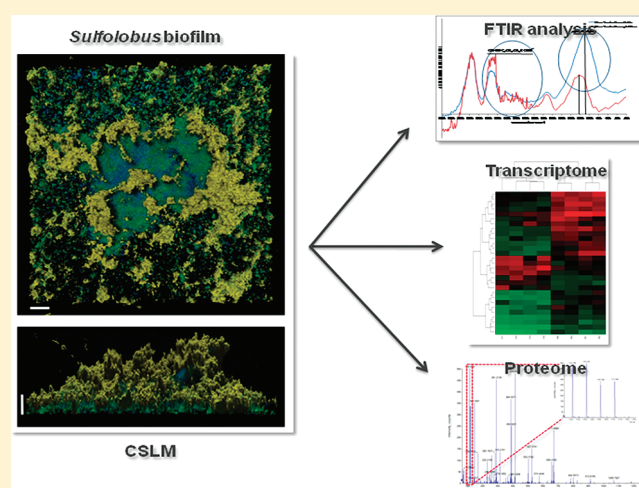
[†]Molecular Biology of Archaea, Max Planck Institute for Terrestrial Microbiology, Karl-von-Frisch-Strasse, 35043 Marburg, Germany

[§]ChELSI Institute, Department of Chemical and Biological Engineering, The University of Sheffield, Mappin Street, Sheffield, S1 3JD, United Kingdom

S Supporting Information

ABSTRACT: Microorganisms in nature often live in surface-associated sessile communities, encased in a self-produced matrix, referred to as biofilms. Biofilms have been well studied in bacteria but in a limited way for archaea. We have recently characterized biofilm formation in three closely related hyperthermophilic crenarchaeotes: *Sulfolobus acidocaldarius*, *S. solfataricus*, and *S. tokodaii*. These strains form different communities ranging from simple carpet structures in *S. solfataricus* to high density tower-like structures in *S. acidocaldarius* under static condition. Here, we combine spectroscopic, proteomic, and transcriptomic analyses to describe physiological and regulatory features associated with biofilms. Spectroscopic analysis reveals that in comparison to planktonic life-style, biofilm life-style has distinctive influence on the physiology of each *Sulfolobus* spp. Proteomic and transcriptomic data show that biofilm-forming life-style is strain specific (eg ca. 15% of the *S. acidocaldarius* genes were differently expressed, *S. solfataricus* and *S. tokodaii* had ~3.4 and ~1%, respectively). The -omic data showed that regulated ORFs were widely distributed in basic cellular functions, including surface modifications. Several regulated genes are common to biofilm-forming cells in all three species. One of the most striking common response genes include putative Lrs14-like transcriptional regulators, indicating their possible roles as a key regulatory factor in biofilm development.

KEYWORDS: archaea, sulfolobus, biofilm, proteomics, transcriptomics, FTIR, thermophilic, acidophilic



INTRODUCTION

It is now broadly recognized that microorganisms in their natural environments are most often found in surface-associated sessile communities, known as biofilms. This multicellular behavior offers the community members benefits, particularly with regard to increased resistance against environmental fluctuations such as temperature, pH and nutrient availability.¹ The underlying mechanisms behind biofilm formation and its importance for microbial survival in natural habitats have attracted increasing interest. Bacterial model biofilm studies have identified many phenotypes and have provided information on numerous of factors that are important during biofilm development and could be of widespread relevance beyond their importance in model systems. Among these factors are cell-to-cell communication, cell attachment mechanisms, cell-to-cell interconnecting components, surface-associated spreading mechanisms, dispersion mechanisms and genetic elements related to the regulation of biofilm development.

Although archaea are frequently detected in biofilm communities in a wide variety of environments,^{2,3} limited information is available describing biofilm formation in this domain of life. The first archaeal biofilm was described for the hyperthermophilic euryarchaeon *Thermococcus litoralis*. The *T. litoralis* biofilm developed in rich media on hydrophilic surfaces, for example, polycarbonate filters, and was accompanied by mannose-type extracellular polysaccharides production.⁴ The hyperthermophile *Pyrococcus furiosus* was shown to attach to surfaces of mica and carbon coated electron microscopy grids. During this process, the flagella of the cells formed cablelike structures.⁵ Additionally, *P. furiosus* adherence to glass was only possible by cocolonization with *Methanopyrus kandlerii* by using its flagella and establishing cell-to-cell contacts.⁶ For *Archaeoglobus fulgidus*,

Received: April 1, 2011

Published: July 18, 2011

biofilm formation increased in response to unfavorable environmental conditions, including high metal concentrations, pH, and temperature changes.⁷ Recently, biofilm characterization was carried out in the mesoacidophilic archaeon *Ferroplasma acid-armanus*. This euryarchaeon is predominantly found in biofilm-associated structures in the environment, and two distinct biofilm morphologies were described: a multilayer film that formed on both an inert glass as well as pyrite that acts as energy source and 5 mm-long filaments that formed on the sintered glass spargers in a gas lift bioreactor. Proteomic studies on these biofilms showed that 6 out of the 10 up-regulated proteins were involved in the adaptation to anaerobic growth indicating anaerobic zones in the multilayered *Ferroplasma* biofilms.⁸

We have chosen the crenarchaeal model organism *Sulfolobus* spp. to initiate comprehensive studies on archaeal biofilms. *Sulfolobus* species are hyperthermoacidophiles growing optimally at 70–85 °C and pH 2–3 that are found worldwide in geothermally active environments such as solfataric fields. Our previous work has provided evidence that cell surface structures such as flagella and pili are essential for the initial attachment of *Sulfolobus solfataricus* to abiotic surfaces from shaking cultures.⁹ Furthermore, by means of a microtiter plate assay adapted to high temperatures, we established that biofilm formation occurs more broadly in *S. acidocaldarius*, *S. solfataricus* and *S. tokodaii*. Additionally, it was determined that *S. acidocaldarius* most readily engaged in biofilm formation in comparison to the other investigated *Sulfolobus* strains. Confocal laser scanning microscopy showed that the three strains form very different community morphologies, ranging from simple carpet structures in *S. solfataricus* to high density tower-like forming structures in *S. acidocaldarius*. Lectin staining indicated that all three strains produced extracellular polysaccharides containing glucose, galactose, mannose and *N*-acetylglucosamine once biofilm formation was initiated. Whereas flagella mutants showed no phenotype in three day old static biofilms of *S. solfataricus*, a UV induced pili deletion mutant showed biofilm impairment.¹⁰

Bacterial biofilms have previously been examined using transcriptomic, proteomic and *in vivo* expression approaches for *Escherichia coli* and *Pseudomonas* spp.^{11–13} To date, it has been demonstrated that the transition from a planktonic lifestyle to a sedentary biofilm lifestyle requires the coordinated regulation of genes involved in the development of biofilms. These functional genomics analyses have revealed that hundred genes, most of which are uncharacterized, are differentially expressed during sessile lifestyle.^{12,14,15} However, after comparison of the differentially expressed gene sets identified in several recent DNA microarray studies, a common expression pattern for biofilms has yet to emerge, highlighting the particularity of biofilm physiology among the different studied models.^{11,14,16} Proteomics has also supplied a broader perspective on gene expression and has been used successfully to study biofilms.^{17–20} Recently, a combined approach including proteomic and Fourier transform infrared (FT-IR) spectroscopy analysis immensely assisted the investigation of the distinctiveness of biofilm formation in *Bordetella pertussis*²¹ and *E. coli*.²⁰ These studies have both demonstrated that biofilm formation is a rather complex but distinct process and that deep insights into the biofilm physiology can be provided by the combined use of whole cell metabolic fingerprinting by FT-IR, multivariate statistical analysis, and proteomics.^{20,21}

Here, we have carried out a comparative study of three *Sulfolobus* strains (*S. acidocaldarius*, *S. solfataricus* and *S. tokodaii*) to gain insights into the physiological adjustments that may take

place when these archaeons are grown as biofilms. We used a combination of spectroscopic, proteomic and transcriptomic approaches to describe physiological and regulatory features involved in the biofilm lifestyle for each strain. Furthermore, we present the data as a comparative analysis, to highlight common features in biofilm formation among the three *Sulfolobus* strains under study.

EXPERIMENTAL PROCEDURES

Strains and Growth Conditions

The shaking precultures of *Sulfolobus* strains *Sulfolobus solfataricus* P2 (DSM1617), *Sulfolobus acidocaldarius* (DSM639) and *Sulfolobus tokodaii* (DSM16993) were grown for two days aerobically at 76 °C. The media described by Brock et al. (1972) were adjusted with sulphuric acid to a pH of 3 and supplemented with 0.1% w/v tryptone.

Biofilm Growth and Cell Harvesting

Biofilms of the *Sulfolobus* strains were grown in large Petri dishes (150/20 mm gamma-sterile with Ventilation Cams, Sarstedt, Nümbrecht) for two days in Brock media as a standing culture. Four biological replicates were performed for each of the three strains. For all three strains, as was determined by Koerdt et al. (2010), different OD₆₀₀ inoculations were used: for *S. solfataricus* an OD of 0.03, for *S. acidocaldarius* an OD of 0.01, and for *S. tokodaii* an OD of 0.06. The Petri dishes were put in a specially designed metal box (25 cm L × 20 cm W × 20 cm D) with ~500 mL of water in the bottom to minimize evaporation of the media, as described by Koerdt et al. (2010).

After 48 h the planktonic and the biofilm cells were harvested. The supernatant of the Petri dishes containing the planktonic cells was carefully removed. The biofilm was washed with 50 mL of Brock media. Then, 15 mL Brock media was added and the biofilm was harvested with a cell scraper (Cell Scraper, 28 cm length, Greiner bio-one, Frickenhausen). The biofilm and planktonic cells were spun down for 20 min at 4 °C and 2000 × g. The liquid supernatant was removed and the pellets were frozen in liquid nitrogen and stored at –80 °C.

Fourier Transformation Infrared Spectroscopy

Fourier transformation infrared spectroscopy (FTIR) spectroscopy was conducted using a diamond Attenuated Total Reflectance (ATR) apparatus (Pike Technologies, Madison, WI) attached to a Shimadzu IRPrestige-21 Fourier Transformation Infrared Spectrophotometer (Shimadzu, U.K.). A blank spectrum, using the ATR without any biological samples, was run as a background and the baseline shift of the spectra was corrected using the IR solution software provided with the Shimadzu instrument. For each biological sample (biofilm or planktonic), a small amount of the cell biomass was mounted on the ATR, covering the entire diamond surface, and allowed to dry at room temperature before analysis. At least 64 scans, with resolution of 4 cm⁻¹ using the Happ-Genzel apodization function, were collected for all samples.

As biological macromolecules show characteristic peak absorbance between 800 and 1800 cm⁻¹,²² further spectral processing, including atmospheric correction was focused in this region. Spectral processing was carried out using IR solution software and each significant peak was interpreted using the software “Knowitall” (<http://www.knowitall.com/academic/welcome.asp>) and corresponding absorption band assignments for functional groups of macromolecules previously reported for bacteria.

Statistical analysis was carried out for all three strains grown planktonically and as a biofilm using Principal Component Analysis (PCA), using the XLSTAT software (<http://www.xlstat.com/>). Each biological sample was analyzed 5 times to assess technical variations.

X-ray Photoelectron Spectroscopy (XPS) Analysis

XPS analysis was performed as described elsewhere.²³ *Sulfolobus* cells grown planktonically or as a biofilm, were washed twice by centrifugation at $5000 \times g$ for 10 min with demineralised water. The pellets were resuspended in water, freeze-dried under sterile conditions and then mounted onto glass coverslips. The samples with the coverslips were mounted on standard sample studs (sample holder) for analysis. The XPS measurements were carried out on a KRATOS AXIS 165 Ultra Photoelectron spectrometer at 10 kV and 20 mA using the Al K α X-ray source (1486.6 eV). The takeoff angle was adjusted at 90° and data was collected for each sample at three random selected locations (technical replicates). The area corresponding to each acquisition was 400 μm in diameter. A survey scan was initially carried out (pass energy 20 eV, 1.0 eV step size) for C, O and N, followed by a high resolution scan (pass energy 20 eV, 0.1 eV step size) for C and O. Deconvolution of the high resolution scan enables the local chemical bond environments between C and O to be investigated. The binding energies of the peaks were determined using the C1s peak at 284.5 eV. CasaXPS 2.3.12 software was used to carry out the spectral integration.²³ Elemental composition was expressed as atomic concentration. All measurements were conducted in triplicate.

Protein Extraction and iTRAQ Labeling

Independent biological duplicate cells from three different species harvested as described above were washed twice with cold water before being resuspended in 0.5 M TEAB iTRAQ buffer containing 0.1% SDS. Cells were then lysed using ultrasonication (Sonifier 450, Branson) 4 times (alternatively 1 min on ice) at 70% duty cycle, as described in detail elsewhere²⁴ before centrifugation first at $3000 \times g$ for 5 min at 4 °C and then at $21,000g$ at 4 °C for 15 min. Supernatants were subsequently collected as extracted proteins. Total protein concentrations were determined using the RC-DC protein quantification assay (Bio-Rad, U.K.). 100 μg protein (for each phenotype) was used for iTRAQ 4-plex analysis. Proteins were reduced, alkylated, digested and labeled with iTRAQ reagents as described elsewhere.²⁴ Biological duplicates were used for all three *Sulfolobus* species, and for each phenotype (biofilm and planktonic). The iTRAQ labeling of all samples is shown in Table S2 (Supporting Information). Labeled peptides (for each species) were subsequently combined before being dried in a vacuum concentrator.

Labeled Peptides Separation, Mass Spectrometry and Data Analyses

All dried labeled peptide samples were cleaned and fractionated using strong cation exchange on a BioLC HPLC system (Dionex, UK) as detailed elsewhere.²⁴ Labeled iTRAQ peptides were collected every minute, and then dried under vacuum. Selected dried labeled peptides were resuspended in 50 μL of buffer A containing 0.1% formic acid and 3% acetonitrile before submission to a QStar XL Hybrid ESI Quadrupole time-of-flight tandem mass spectrometer, ESI-qQ-TOF-MS/MS (Applied Biosystems/MDS Sciex, Canada), coupled with a nano-LC system (LC Packings Ultimate 3000, Dionex, U.K.). Mass

spectrometry was performed as described previously.²⁴ The sample was separated on a PepMap C-18 reversed phase capillary column (LC Packings) at a flow rate of 3 $\mu\text{L}/\text{min}$, and a gradient was generated by variation of the percentage of buffer B (0.1% formic acid and 97% acetonitrile). The mass detector range was set to 350 to 1800 m/z and operated in the positive ion mode. Peptides with +2, +3, and +4 charge states were selected for fragmentation.

All raw mass spectrometry data were converted into MGF format using the mascot.dll script (V1.6) coupled with Analyst QS 2.0 (Applied Biosystems), before submission to an in-house search algorithm Phenyx V 2.6 (Genebio, Geneva) (see Pham et al.,²⁵ for more detail) with the *Sulfolobus solfataricus* P2, *Sulfolobus acidocaldarius*, *Sulfolobus tokodaii* databases downloaded from NCBI (<http://www.ncbi.nlm.nih.gov/Ftp/>) in Jan 2009. The search parameters were set as follows: peptide tolerance 0.4 Da, charge +2,+3 and +4, min peptide length, z-score, max p-value and AC score were 5, 5.5, 10^{-6} and 5.5 respectively, and enzymes used for searching were trypsin, with up to two missed cleavages. Modifications were analyzed as follows: 4-plex iTRAQ mass shifts (+144 Da, K and N-term), methylthiol (+46 Da) and oxidation of methionine (+16 Da). Data were then exported to Excel (Microsoft 2008, Redmond, WA) for further analysis. Furthermore, the false positive rates (FPR) were also performed by searching data with the reversed databases of these *Sulfolobus* spp., and calculated as the following equation: $\text{FPR} = (2 \times \text{decoy_hits} * 100\%) / (\text{decoy_hits} + \text{true_hits})$.

The quantification of identified proteins was performed based on methods described previously by Pham, et al. (2010), and a rigorous statistical method, including multiple test correction, was also applied to choose significantly regulated proteins for biological discussions (see also Pham, et al.²⁵ for full details of methods). First, protein quantification was calculated by the geometric means of the ion reporters' intensities (at least 2 peptides for each protein) before a *t* test comparison (with $\alpha = 0.05$) between the reporter ions' intensities was performed, followed by a Bonferroni correction. Furthermore, proteins were considered as regulated ones when all *t* tests of these proteins were less than a value of α/P (Bonferroni correction) (P : number of quantified proteins).

RNA-Isolation

The cell pellet was resuspended in 1 mL ice-cold AE-buffer (20 mM sodium-acetate, pH 5.5; 1 mM EDTA) and then centrifuged for 5 min at 4 °C. The pellet was resuspended in 600 μL AE-buffer. Subsequently, 900 μL of hot phenol-chloroform-isoamyl alcohol (25:24:1, 60 °C) and 10 μL 25% SDS (w/v) were added. The suspension was incubated for 15 min at 60 °C and every 2–3 min the tube was inverted. The tube was incubated for 20–30 min on ice and then centrifuged at $15\,700 \times g$ for 30 min at 4 °C. In a new phase lock tube (Phase Lock Gel Light 2 mL, 5 PRIME, Hamburg), one volume of phenol-chloroform-isoamyl alcohol and 62.5 μL 2 M sodium-acetate were added to the supernatant. After centrifugation $15\,700 \times g$ for 15 min at 4 °C the supernatant was transferred in a new 2 mL tube, 2.5 volumes of 96% ethanol was added and incubated for 1–2 days at -80 °C. The samples were thawed on ice and centrifuged for 30 min at 4 °C. After washing the pellet twice with 500 μL of 70% ethanol, the pellet was air-dried at room temperature. Finally the pellet was resuspended in 100 μL RNase free water (Qiagen, Hilden). The RNA isolation was

controlled via Nanodrop (NanoDrop ND-1000 Peqlab, Erlangen) and analytical gel electrophoresis. To remove all DNA, the samples were digested with DNase (TURBO DNA-free, Ambion Applied Biosystems, Darmstadt) according to the manual. Additionally RNase Inhibitor (RNasin Plus RNase Inhibitor, Promega, Mannheim) was added to inhibit the digestion of RNA. The purity of the RNA was tested via PCR with primers for a very small product before and after DNA digestion.

Microarrays Experiments and Statistical Analysis

Four biological replicates per strain were measured both for biofilm and nonbiofilm grown cells. Geniom Biochips containing 4 arrays were used for the analysis. Each array on the chip had 15 000 spots with 50mer probes. For each gene, five to six different probes were computed. The probe computation relies on freely available information of the DoE Joint Genome Institute. For background correction single "T" nucleotide probes were used. For further verifications, additional hybridization controls were added to the array template. Blank, labeling control and hybridization control probes are not included in the data.

Febit (company, Heidelberg) used the MessageAmpII-Bacteria Prokaryotic RNA Kit from Ambion for the labeling of RNA for mRNA expression analysis. The kit provides a transcription of RNA in cDNA, following a transcription in cRNA while enrichment of all nucleic acid molecules is included. For each array, 1 μ g of total RNA was labeled according to the manufacturer's instructions. After labeling, samples were dried in a vacuum concentrator and fragmented with a fragmentation buffer (see Febit protocol 20). Finally, Febit's proprietary standard Hybridization Buffer (20 μ L per array) was added. Hybridization was done automatically overnight (16 h) at 45 °C using the Geniom RT analyzer. After hybridization, the Geniom Biochip was washed automatically. For maximum sensitivity, Febit used biotin and its detection with streptavidin-phycoerythrin (SAPE), in combination with Febit's Consecutive Signal Enhancement (CSE) procedure. For a more detailed description please read Febit protocol 010. The feature recognition (using Cy3 filter set) and signal calculation were done automatically within milliseconds. Accurate detection of mRNA profiles correlates well with the qPCR data. There was no photo bleaching, thus enabling repeated measurements and multiple detection of each Biochip.

The basis of the analysis was Febit's background corrected data sets. In these data sets, all negative values were replaced by 0. To reduce influences of sample binding problems, only the three spots with the highest intensities were used per gene in the following calculations. For each array the sum of all intensities was calculated. Subsequently all intensities of each array were multiplied with a factor to level the total sum to the highest. Afterward, the three intensities of each gene were reduced to the median, followed by quantile normalization. The following calculations were done in Microsoft Excel.

The medians of the four biological replicates for biofilm and planktonic cells were calculated and their logarithmic fold change calculated to the base 2. The significance was computed by a statistical heteroscedastic *t* test with a two-tailed distribution. Regulated genes were chosen by a specific threshold value for each strain. For *S. acidocaldarius*, the standard threshold value of 0.05 was selected. For the two other strains, the values were adapted by the average of the calculated significances (*S. solfataricus* 0.0631, *S. tokodaii* 0.0747). The resulting significantly regulated genes were split in two groups (up-, down-regulated).

To find homologues for both groups, databases containing the amino acid sequences were created. Afterward, for each gene, a BLAST search in the specific database was performed with a cutoff value of e^{-10} .

Quantitative RT-PCR (qRT-PCR)

The cDNA Synthesis was performed with the iScript cDNA Synthesis Kit (Bio-Rad, Munich) according to the manual. qPCR was performed using SYBR Green qPCR Master Mix (Fermentas, St. Leon-Rot). Two-step cycling qPCR was carried out in 25 μ L final volume reaction according to the provider indications. A 20 times diluted cDNA of four biological replicates per strain were assayed both for biofilm and nonbiofilm grown cells. Reactions were set up in a 7300/7500 Real Time PCR Systems Cyclor (Applied Biosystems, Darmstadt Germany). Primers were designed to amplify a specific product of a length range of 90–120 bp (oligonucleotide sequences are listed in Table S4 in the Supporting Information section). All primers were used at the final concentration of 0.3 μ M. The cycling program used for each primer pair was as follows: 10 min at 95 °C, 40 cycles of 15 s at 95 °C and 60 s at 60 °C (annealing and extension in one step). *Saci_0269*, *SSO0007* and *ST2326* genes were used as standards for the relative quantification. The Ct values were calculated automatically using software core application version 1.2.3 (Applied Biosystems).

RESULTS

Spectroscopic Analysis of Biofilm versus Planktonic Cells

Fourier Transform Infrared Spectroscopy (FT-IR) and X-ray Photoelectron Spectroscopy (XPS) Analysis. FT-IR spectroscopy has been successfully used as a rapid nondestructive technique to characterize the molecular composition of many different microbial systems,^{26–29} including environmental isolates³⁰ and biofilms.^{20,30,31} ATR-FTIR can detect both surface and cytoplasmic constituents of a biological sample. Furthermore, Jiang et al.²⁹ established that variations in the ATR-IR spectrum essentially arose due to modifications on the cell surface. Therefore, it is proposed that any variations observed in the ATR-IR spectra conducted in this study, can be related to surface specific changes in functional groups.

FT-IR spectra between 800 and 1800 cm^{-1} were recorded from *S. acidocaldarius*, *S. solfataricus* and *S. tokodaii* cell samples grown either in the biofilm or planktonic mode, respectively (Figure 1). Principal component analysis (PCA) of the FT-IR spectra was applied to interpret the variations among the three strains in both lifestyles (biofilm v/s planktonic). PCA analysis showed that cells associated with biofilms clustered separately from their respective planktonic counterparts for each investigated strain (see Figure S1 in Supporting Information). These findings suggest that the FT-IR data provides spectroscopic evidence to support the premise that *Sulfolobus spp.* biofilm population has characteristics that distinguish it from the planktonic cells population.

To further investigate the potential chemical functional groups within the FT-IR spectrum that may have contributed to the observed differences in the PCA analysis, chemical functional groups were assigned to the FT-IR spectra (Figure 1) according to definitions from Eboigbodin and Biggs,²⁶ Naumann²² and Bosch et al.³² Comparative analysis of normalized spectral data (Figure 1) mainly revealed a significant increase in the intensity of absorption bands assigned to carbohydrate functional groups

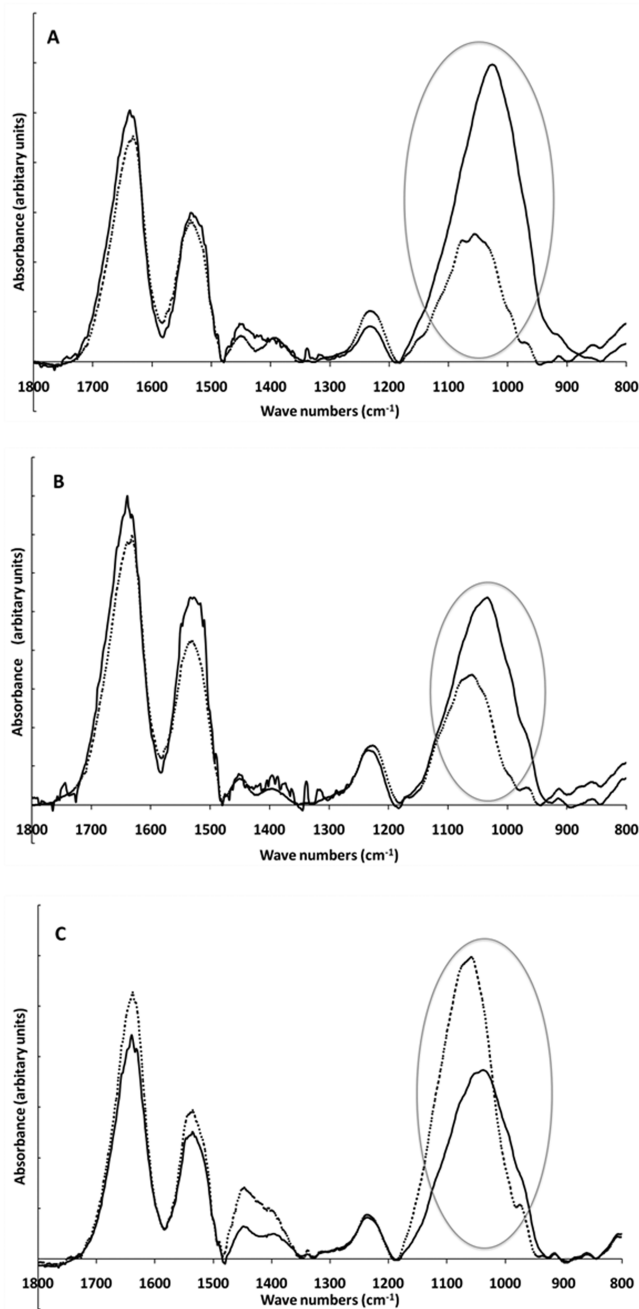


Figure 1. Overlay of normalized spectra FTIR data of (A) *S. acidocaldarius*, (B) *S. solfataricus* and (C) *S. tokodaii* grown either as biofilm (solid line) or planktonically (dotted line). Spectra are baseline corrected and normalized to 2930 cm^{-1} .

(spectral region: $900\text{ to }1200\text{ cm}^{-1}$) in biofilm cells of both *S. acidocaldarius* (Figure 1A) and *S. solfataricus* (Figure 1B) strains in comparison to their planktonic counterparts. However, despite the same normalization across all strains, the significant increase in absorption band intensity in carbohydrate region of *S. tokodaii* biofilm cells compared to planktonic cells was not found (Figure 1C). Moreover, additional specific banding assignment for chemical function groups was difficult in this region ($1200\text{ and }900\text{ cm}^{-1}$), as it is made up of vibrations corresponding to the stretching of diverse polysaccharides groups.²³

Additionally, XPS analysis was performed to further describe the cell surface chemical composition in all three *Sulfolobus* spp.

XPS analysis allows for the quantification of the elemental surface composition and to assess the local chemical environment of carbon, oxygen and nitrogen atoms on the cell surface. XPS wide scan data (see Figure S2 and Table S1 in the Supporting Information) showed that the cell surface (approximately $1\text{--}10\text{ nm}$ in depth) was mainly comprised of C, N, O.

The abundance of C, N, O was therefore estimated for each *Sulfolobus* strains and in comparison between biofilm-associated cells and planktonic cells samples. N/C and O/C atomic concentration ratios indicate the fraction of carbon linked to either nitrogen or oxygen atoms on the cell surface, respectively (Table 1). The results indicated an excess of O/C linkages on the cell surface of all three strains (Table 1). Furthermore, when compared to planktonic cell samples, an increase in the O/C ratios was determined for biofilm-associated cells of *S. acidocaldarius* and *S. solfataricus*. The opposite was found in the *S. tokodaii* biofilm cell surface (Table 1). Since polysaccharides predominantly contain O/C linkages in their structures, this ratio might be attributed to an increase in polysaccharide moieties. Moreover, O/C ratios were found to be higher than N/C ratios, indicating that O/C ratios might arise from polysaccharide moieties rather than from the amide linkages (C-NHCO-C) on the protein moieties (Table 1), as a 1:1 ratio (approx.) between O/C and N/C values is expected for a proteinaceous cell surface.

Thus, the XPS analysis correlated with the FT-IR spectra in that a statistically significant increase was determined in the polysaccharide moieties on the *S. acidocaldarius* and *S. solfataricus* biofilm cell surfaces. The opposite trend was determined in the *S. tokodaii* biofilm cell surface (Table 1). Using both FTIR and XPS, differences between biofilm and planktonic modes of growth in all three *Sulfolobus* species were noted, which is most likely due to changes in the carbohydrate composition.

Comparative Proteomic Analysis of Biofilm versus Planktonic Cells

Taking the spectroscopic evidence that *Sulfolobus* biofilm population shows distinctive features in comparison to the free-living cells, we further assessed the impact of this mode of growth on the proteome of *Sulfolobus* species. Total protein extracts of *S. acidocaldarius*, *S. solfataricus* and *S. tokodaii* from biofilm-associated and planktonic populations were comparatively analyzed using iTRAQ. Planktonic and biofilm cell samples of each strain at the same time (2 days of growth) were used in the proteomic experiments. Using the Phenix program for searching within correlated databases, 11063, 10122, and 11419 peptides corresponding to 481, 463, and 542 quantified proteins (≥ 2 peptides) were identified for *S. solfataricus*, *S. acidocaldarius*, and *S. tokodaii*, respectively (see sheet 1 for details of peptides lists and sheet 2 for details of quantified proteins lists in proteomics Supporting Information section, Excel files 1, 2, and 3). Furthermore, false positive rates of 0.25%, 0.18% and 0.31% were also estimated for *S. solfataricus*, *S. acidocaldarius*, and *S. tokodaii*, respectively, as described in Experimental procedures section. The numbers of all significantly regulated proteins are summarized in Table S3 (Supporting Information section). Since two biological replicates for each condition (biofilm (iTRAQ labels 116 and 117) and planktonic (iTRAQ labels 114 and 115) for each *Sulfolobus* strain) were carried out, four *t* tests were calculated for each *Sulfolobus* species. To pick up regulated proteins, we required all *t* test values of these proteins to be less than a value of α/P (Bonferroni correction) (where $\alpha = 0.05$ and

Table 1. Quantification of the Elemental Surface Composition (C, O and N) of *S. acidocaldarius* (S.aci), *S. solfataricus* (S.so) and *S. tokodaii* (S.to) Grown Planktonically and as Biofilm^a

	planktonic cells			biofilm cells		
	S. aci	S. so	S. to	S. aci	S. so	S. to
C	62.23 ± 1.36	63.73 ± 1.10	52.97 ± 1.42	57.42 ± 0.74	59.53 ± 0.56	56.22 ± 2.41
O	29.90 ± 0.17	28.38 ± 1.49	40.81 ± 2.81	34.50 ± 1.04	31.36 ± 0.40	35.49 ± 2.43
N	7.88 ± 1.20	7.90 ± 0.40	6.23 ± 1.39	8.09 ± 0.30	9.12 ± 0.16	8.29 ± 0.03
N/C	0.13 ± 0.02	0.120 ± 0.004 ^Δ	0.12 ± 0.02	0.140 ± 0.003	0.150 ± 0.004 ^Δ	0.15 ± 0.01
O/C	0.48 ± 0.0f	0.45 ± 0.03 ^β	0.77 ± 0.07 ^γ	0.60 ± 0.03 ^α	0.53 ± 0.01 ^β	0.63 ± 0.07 ^γ

^a Numbers with similar Greek symbols are statistically significant (90% confidence interval; Students' *t* test, $p < 0.1$). Outliers were detected and removed in the data by calculating the interquartile range and also by using Grubbs' test at 99% confidence interval.

P is number of quantified proteins). As a result, values of 1.04×10^{-4} , 1.08×10^{-4} and 9.24×10^{-5} were calculated for *S. solfataricus* P2, *S. acidocaldarius*, *S. tokodaii*, respectively. However, we also considered proteins with p -values ≤ 0.05 regulated proteins for a confirmatory test. Lists of significantly regulated proteins are summarized in sheet 3 in proteomics Supporting Information, Excel files 1, 2, and 3 for *S. solfataricus*, *S. acidocaldarius*, *S. tokodaii*, respectively. In order to get a wider view for understanding the behavior of cells in biofilm versus planktonic conditions, proteins with p -values less than $\alpha = 0.05$ (without correction) (known as lists of potentially regulated proteins) were also used for further discussion. The lists of these potentially regulated proteins are shown in the sheet 4 in proteomics Supporting Information, Excel files 1, 2 and 3.

In terms of identifying proteins that were differentially changed during the biofilm mode of life versus the planktonic counterparts, a protein comparison was performed. *S. acidocaldarius* had 30 biofilm-regulated proteins (19 up- and 11 down-regulated), *S. solfataricus* displayed 36 protein changes (17 up- and 19 down-regulated) and for *S. tokodaii* 67 proteins changed their relative abundances in the biofilm lifestyle (41 up- and 26 down-regulated). All the statistically significant changes are tabulated in Table S3 in the Supporting Information section. The most noteworthy findings are listed in Tables 2 and 3 and discussed in the next section. Additionally, a BLASTp analysis was carried out in order to identify common biofilm-regulated proteins between the three *Sulfolobus* species (biofilm core response). Amino acid sequences as queries of both significantly up-regulated proteins and down-regulated proteins were used in this analysis, respectively. This analysis yielded three different proteins which were commonly up-regulated, while four proteins were found to be down-regulated in all three *Sulfolobus* species (Figure 2, Table 2). Furthermore, the BLASTp analysis also yielded homologous proteins that were commonly regulated in at least two strains (Figure 2, Table 3).

Identification of Differentially Expressed Proteins in Biofilm-Grown *Sulfolobus* Strains

Identified proteins were categorized in functional groups using the assigned COG numbers. By means of this analysis, we were able to find that *Sulfolobus* spp. biofilm mode of growth altered not only the expression of proteins involved predominantly in cellular functions like energy production, energy conversion, adaptation to environmental changes and stress, and substrate transport/binding activities but also the expression of proteins implicated in cellular processes and regulatory events (Table 3).

Table 2. Common Biofilm-Regulated Proteins and Genes within *S. acidocaldarius*, *S. solfataricus* and *S. tokodaii* Strains

Up-regulated in biofilm		
proteomic analysis annotation	ORF number	fold change (log ₂)
transcriptional regulator	Saci_1223	0.85
Lrs14-like protein	SSO1101	1.48
	ST0837	0.82
DNA-binding protein	Saci_0064	1.02
	SSO10610	1.0
	STS077	0.26
Chaperone	Saci_1665	0.79
Small heat shock protein	SSO2427	0.88
hsp20	ST0555	0.58
RNA microarray analysis		
ABC transporter ATP-binding protein	Saci_2305	0.91
	SSO0053	0.74
	ST0535	0.22
Down-regulated in biofilm		
proteomic analysis annotation	ORF number	fold change
Thermosome		
-alpha subunit (thsA)	Saci_1401	-0.24
	SSO0862	-0.67
	ST1253	-0.14
-beta subunit (thsB)	Saci_0666	-0.4
	SSO0282	-0.43
	ST0321	-0.16
-gamma subunit	Saci_1203	-0.63
	SSO3000	-0.43
	ST0820	-0.37
V-type ATPase	Saci_1548	-0.55
	SSO0563	-1.03
	ST1436	-0.47
RNA microarray analysis		
3-oxoacyl-(acyl carrier protein) reductase (fabG-1)	Saci_1792	-1.72
	SSO0975	-0.64
	ST1299	-0.21

Proteomic data showed that adjustments in energetic metabolism are made during growth in a biofilm. Putative cytochrome oxidase subunits were identified as up-regulated in *S. solfataricus*

Table 3. Selected Up- and Down-regulated Genes and Proteins between *S. acidocaldarius*, *S. solfataricus* and *S. tokodaii* during Biofilm Mode of Growth^a

functional group	ORF	fold change (log ₂)		p-value
		proteomic	microarray	microarray
Energy production and conversion				
Cytochrome c oxidase polypeptide I	Saci_0097	n.d.	1.31	0.006
	ST2595	n.s.	0.9	0.017
Cytochrome b558/566, subunit A	SSO2801	1.41	n.d.	
Cytochrome b	ST0137	0.43	n.s.	
Rieske iron–sulfur protein (SoxL)	Saci_1860	n.d.	2.57	0.001
Quinol oxidase-2, sulfocyanin (SoxE)	SSO2972	n.d.	0.59	0.034
V-type ATP synthase subunit B	Saci_1549	−0.35	−0.5	0.006
V-type ATPase, alpha subunit	Saci_1548	−0.55	n.s.	
	SSO0563	−1.03	n.s.	
	ST1436	−0.47	n.s.	
ATP synthase subunit E	SSO0561	1.01	n.s.	
Acetyl-coenzyme A synthetase	Saci_2062	n.d.	0.94	0.025
	ST1803	n.s.	0.76	0.044
Lactate/malate dehydrogenase	Saci_0246	−1.03	n.s.	
Succinyl- CoAsynthetase betasubunit	ST0963	0.54	n.d.	
NADP dependent glyceraldehyde-3-phosphate dehydrogenase	ST2477	−0.61	n.s.	
Phosphoenolpyruvate synthase	Saci_1417	0.56	n.s.	
Acyl-CoA dehydrogenase related protein (acd-like2)	SSO2497	n.d.	0.27	0.051
	ST0085	n.s.	0.69	0.075
Carbon monoxide dehydrogenase subunit G	SSO2430	n.d.	−1.19	0.029
Sulfurtransferase enoyl-CoA hydratase	ST0048	2.01	n.s.	
Carbon monoxide dehydrogenase large chain	Saci_2117	n.s.	−0.51	0.002
	SSO3009	n.d.	−0.3	0.046
Oxidoreductase	SSO2794	n.d.	−0.32	0.021
Thiosulfate reductase electron transport protein (PhsB)	ST1839	n.d.	−0.67	0.022
Pyridine nucleotide-disulfide oxidoreductase	Saci_0331	−1.16	n.s.	
	ST0615	−0.71	n.s.	
Formate dehydrogenase subunit alpha	ST0081	−0.3	n.s.	
Indolepyruvate oxidoreductase, subunit A	ST0732	−0.62	n.s.	
Anaerobic glycerol-3-phosphate dehydrogenase subunit C	ST2369	−0.65	n.s.	
Diphosphomevalonate decarboxylase	Saci_1245	1.08	n.s.	
	ST0977	1.02	n.d.	
Dehydrogenase (flavoprotein)	Saci_0292	0.61	n.s.	
3-hydroxybutyryl-CoA Dehydrogenase	Saci_1109	0.5	n.s.	
Inorganic pyrophosphatase	SSO2390	1.16	n.s.	
Anaerobic dimethylsulfide reductase	ST1789	1.06	n.s.	
Putative thiosulfate sulfurtransferase	ST2564	1.22	n.s.	
Sulfurtransferase enoyl-CoA hydratase	ST0048	2.01	n.s.	
Carbohydrate transport and metabolism				
Sugar-related transporter	Saci_1782	n.d.	−0.59	0.381
	SSO2057	n.d.	−0.93	0.023
Sugar transporter	Saci_2111	n.d.	−0.71	0.006
	SSO2716	n.d.	−0.66	0.012
proline/betaine transporter	SSO2938	n.d.	−0.31	0.056
Maltose-binding protein	ST1103	0.44	n.s.	
Lipid transport and metabolism				
3-oxoacyl-(acyl carrier protein) reductase (fabG-1)	Saci_1792	n.d.	−1.72	0.003
	SSO0975	n.d.	−0.64	0.012
	ST1299	n.d.	−0.21	0.032

Table 3. Continued

functional group	ORF	fold change (\log_2)		<i>p</i> -value
		proteomic	microarray	microarray
4-coumarate-CoA ligase 1	Saci_2207	n.d.	0.79	0.015
	ST1388	n.d.	0.29	0.041
Transport-related proteins				
	SSO2619	0.79	n.s.	
Oligopeptide-binding protein	ST2539	0.28	n.s.	
Permease, major facilitator Superfamily	SSO2701	1.58	n.s.	
Inorganic ion transport and metabolism				
ABC transporter ATP-binding protein	Saci_2305	n.d.	0.91	0.032
	SSO0053	n.d.	0.74	0.031
	ST0535	n.s.	0.22	0.015
ABC transporter, ATP binding subunit	SSO1078	n.s.	0.26	0.61
	ST1577	n.d.	0.2	0.016
Copper transport ATP-binding protein	Saci_2305	n.d.	0.91	0.032
	SSO0053	n.d.	0.74	0.031
	ST0535	n.s.	0.22	0.015
Cation efflux integral membrane protein	Saci_0242	n.d.	0.76	0.022
	ST2110	n.d.	0.28	0.048
Predicted solute binding protein	SSO1273	0.94	0.58	0.033
Transcriptional regulators				
Lrs14 like protein	Saci_1223	0.85	n.d.	
	SSO1101	1.48	n.d.	
	ST0837	0.82	n.s.	
Lrs14 like protein	SSO1108	0.91	n.d.	
Sugar-specific transcriptional regulator	SSO0048	1.24	n.s.	
	ST2050	0.25	n.d.	
Stress-related proteins and chaperones				
Small heat shock protein, hsp20	Saci_1665	0.79	n.s.	
	SSO2427	0.88	n.d.	
	ST0555	0.58	n.s.	
Thermosome Hsp60, alpha subunit	Saci_1401	-0.24	n.s.	
	SSO0862	-0.67	n.d.	
	ST1253	-0.14	n.s.	
Thermosome Hsp60, beta subunit	Saci_0666	-0.4	n.s.	
	SSO0282	-0.43	n.s.	
	ST0321	-0.16	n.s.	
Thermosome (gamma subunit)	Saci_1203	-0.55	-0.68	0.041
	SSO3000	-1.03	-0.15	0.072
	ST0820	-0.47	n.s.	
Thioredoxin	Saci_1823	n.d.	0.88	0.002
	SSO2232	n.d.	0.4	0.039
Peroxioredoxin	Saci_2227	n.d.	0.47	0.05
	SSO2613	n.s.	0.38	0.063
FKBP-type peptidyl-prolyl cis-trans isomerase	SSO0758	-0.36	n.s.	
Bacterioferritin comigratory protein	ST1785	0.33	n.s.	
Universal stress protein	SSO1865	0.74	n.s.	
Cell motility/surface appendages				
Flagella accessory protein J (flaJ)	Saci_1172	n.d.	0.84	0.005
Flagellar accessory protein FlaH	Saci_1174	n.d.	1.42	0.003
Flagellar protein F	Saci_1175	n.d.	0.75	0.001
Hypothetical protein	Saci_1173	n.d.	0.73	0.002
	SSO0119	n.d.	0.54	0.06

Table 3. Continued

functional group	ORF	fold change (log ₂)		p-value
		proteomic	microarray	microarray
UV induced pili system (upsF)	SSO0119	n.d.	0.54	0.06
Surface layer glycoprotein; Flags: Precursor	SSO0389	0.6	n.d.	
Cell wall/membrane/envelope biogenesis				
hypothetical protein	ST2425	n.d.	0.8	0.001
hypothetical protein	SSO2829	n.d.	0,78	0.001
hypothetical protein	Saci_0134	n.d.	0,68	0,001
DNA binding proteins				
Similarity with Sso10 (hypothetical proteins)	Saci_0882	1.11	−0.94	
DNA-binding protein 7 (Sul7d)	Saci_0064	1.02	n.d.	
	SSO10610	1	n.d.	
	STS077	0.26	n.d.	
DNA-binding protein 7	Saci_0362	0.73	n.s.	
	SSO9180	1.02	n.d.	
Chromatin protein Cren7	Saci_1307	0.78	n.d.	
	SSO6901	1.2	n.d.	
Chromatin protein Alba	Saci_1322	0.74	n.s.	
	STS141	0.36	n.d.	
Transcription and translation components				
Methylation guide ribonucleoprotein complex	Saci_1347	0.27	n.s.	
50S ribosomal protein L7Ae	Saci_1520	0.45	n.s.	
	Cell cycle			
ATP-dependent Zn Protease	Saci_0838	0.54	n.s.	
Replication				
Replication factor C small subunit	ST0475	−1	n.s.	
Conserved/hypothetical protein	Saci_0134	n.d.	0.7	0.001
	SSO2829	n.d.	0.78	0
	ST2425	n.d.	0.8	0.002
	Saci_0139	n.d.	−0.75	0.001
	SSO0550	n.d.	−0.56	0.034
Similarity with Sso10	Saci_0882	1.11	n.s.	
	ST0658	0.43	n.d.	
Mn-dependent transcriptional regulator	SSO3242	0.85	n.d.	
Superfamily I DNA and RNA helicases	SSO1456	1.05	n.d.	
Endobeta-mannanase	SSO3007	1.24	n.s.	
Aconitate hydratase	ST0833	0.44	n.s.	
Undecaprenyl pyrophosphate	ST1813	0.53	n.s.	
CRISPR-associated autoregulator, DevR- family	ST0029	−0.42	n.s.	

^a Fold changes correspond to the ratio of biofilm v/s planktonic. Result confidentiality was estimated by *p*-values calculation. *p* ≤ 0.05 was used for all 3 strains in the proteomic analysis. *p*-values of ≤0.05, ≤ 0.0631 and ≤0.0747 were used for *S. acidocaldarius*, *S. solfataricus* and *S. tokodaii* respectively, in the transcriptomic analysis. n.d., not determined; n.s., not significant; −, down-regulated in biofilm.

(SSO2801) and *S. tokodaii* (ST0137) biofilm cells (Table 3). In addition, while V-type ATPase subunit B levels were decreased in *S. acidocaldarius* biofilm cells, V-type ATPase alpha subunit was found to be down-regulated in all three *Sulfolobus* strains biofilm cells (Table 2).

Levels of proteins related to transport functions were altered in biofilm-associated cells of *S. solfataricus* and *S. tokodaii*. A homologous oligopeptide-binding protein (SSO2619 and ST2539) was up-regulated in both strains and a maltose-binding

protein levels (ST1103) were greater in *S. tokodaii* biofilm-associated cells. Moreover, a putative permease (SSO2701) was biofilm-up-regulated in *S. solfataricus* (Table 3). Furthermore, molecular chaperones were regulated during biofilm growth. A small heat shock protein (Hsp20) was found to be commonly biofilm-up-regulated among the three *Sulfolobus* species (Saci_1665 and SSO2447). Additionally, the three thermosome subunits were down-regulated in biofilm-associated cells from each species (Table 2). *S. acidocaldarius* and *S. solfataricus* also displayed up-regulation of two other

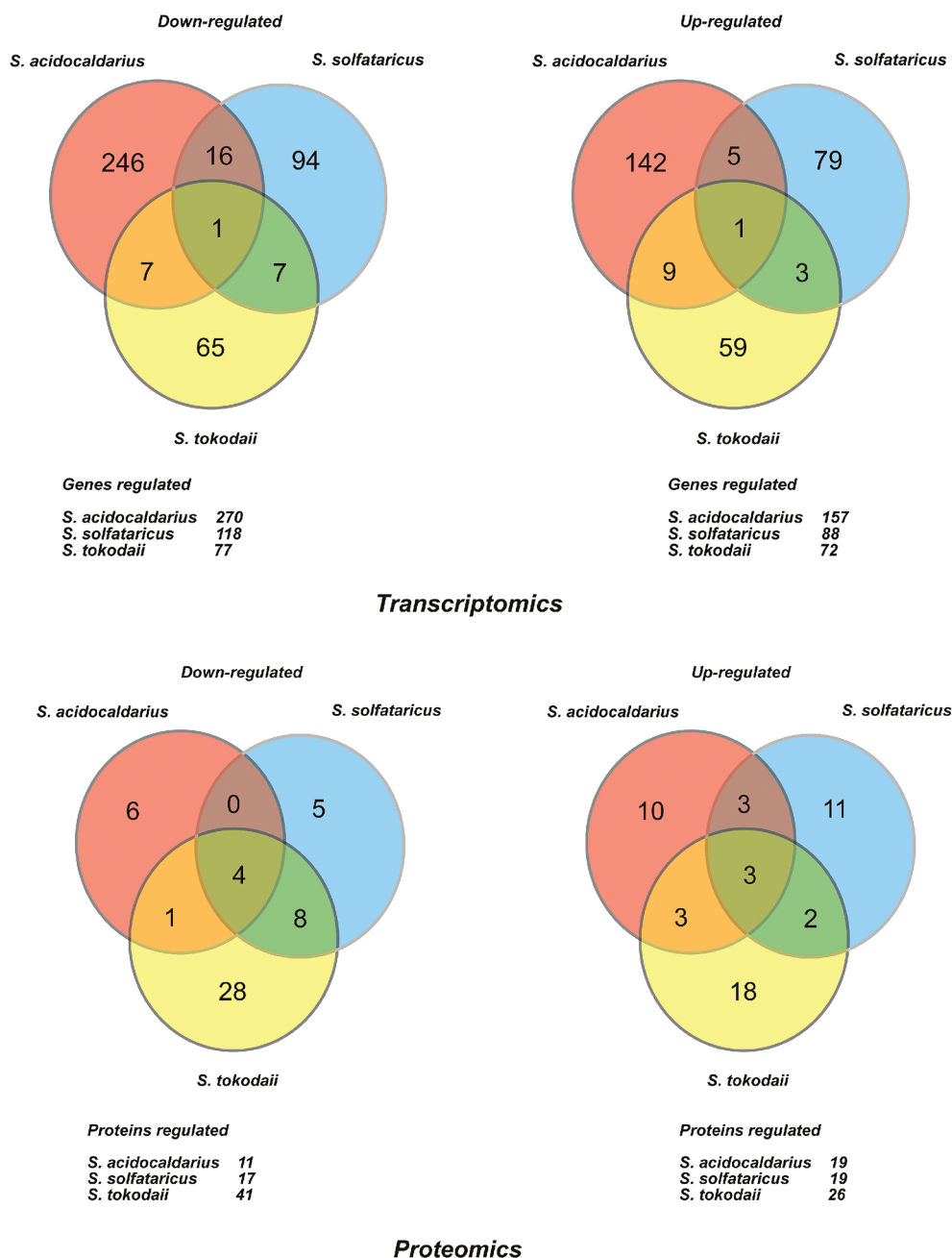


Figure 2. Venn-diagram of (A) transcriptomic and (B) proteomic profiling biofilm response between *Sulfolobus* strains. Up- and down regulated genes and proteins were analyzed by BLASTp in order to identify common biofilm-regulated changes at the transcriptomic and proteomic level. The number of homologous genes and protein between the *Sulfolobus* species are indicated by numbers.

stress-related proteins, that is, a thioredoxin (Saci_1823 and SSO2232) and a peroxiredoxin (Saci_2227 and SSO2613), while *S. tokodaii* showed increased levels of a bacterioferritin comigratory protein-like, belonging to the peroxiredoxins family proteins.³³ As is well-known, peroxiredoxins are ubiquitous proteins that catalyze the reduction of hydroperoxides, which undertake the thiol-dependent reduction of peroxide substrates, thus conferring resistance to oxidative stress.³³

The DNA-binding protein Sul7d (Saci_0064, SSO10610 and STS007) also exhibited altered expression patterns in all three *Sulfolobus* species in biofilm-grown populations. Sul7d has been intensely studied in *S. acidocaldarius* and *S. solfataricus*,

and it is described as an archaeal histone-like protein that binds nonspecifically to DNA inducing negative supercoiling (Baumeister et al.³⁴).

From our BLASTp analyses, we identified a putative transcriptional regulator Lrs14-like that was upregulated in biofilms of all three species (Saci_1223, SSO1101 and ST0837) (Table 2). These putative proteins are homologous to the Lrs14 protein (SSO1108) of *S. solfataricus*, the protein levels of which were also increased during the biofilm lifestyle (Table 3). Thus, the expression of these homologous transcriptional regulators might constitute a key regulatory factor involved in *Sulfolobus* biofilm development. Additionally, the expression of some other genes

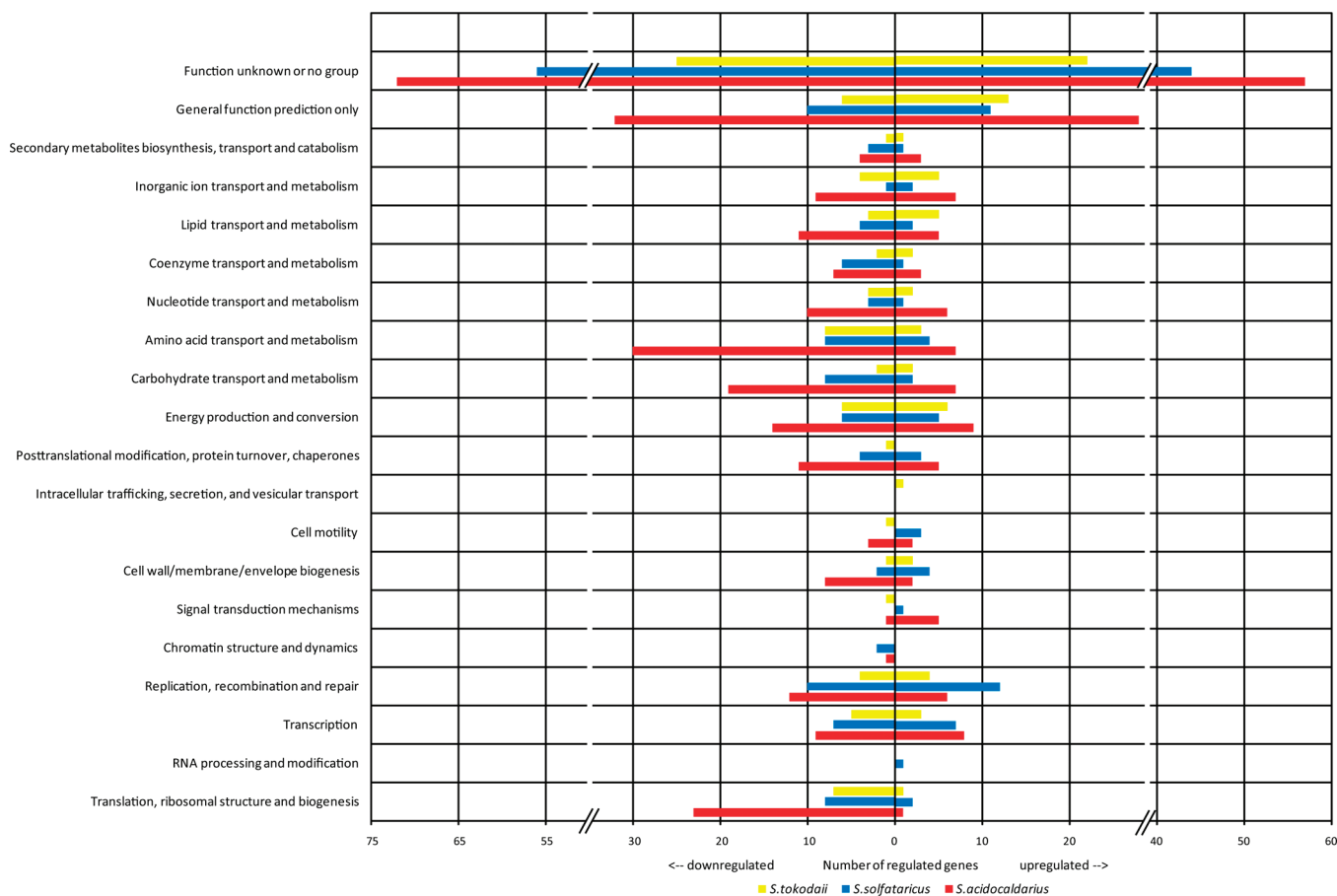


Figure 3. Whole genome expression profiling of *S. acidocaldarius*, *S. solfataricus* and *S. tokodaii* biofilms compared to planktonic cells after 2 days of growth. Genes whose expression levels significantly changed were categorized into functional groups in terms of their COG assigned numbers. The bars show the numbers of genes belonging to each group that were altered in expression (up- and down-regulated).

encoding for homologous Lrs14 proteins were also altered during the biofilm mode of growth, as revealed by qRT-PCR experiments (Table S4, Supporting Information).

Transcriptional Response of Biofilm-Grown *Sulfolobus* Strains

To broaden our analysis from proteomics to include transcriptomics to identify biofilm-regulated genes, the transcriptional profile of *S. acidocaldarius*, *S. solfataricus* and *S. tokodaii* biofilm-associated cells was compared to that of their planktonic counterparts using microarray analysis. Results from the microarrays indicates that the expression of 437, 244, and 152 transcripts changed significantly for *S. acidocaldarius*, *S. solfataricus* and *S. tokodaii*, respectively, during the establishment of a two day old biofilm (Supporting Information, Excel file “Transcriptomic significant data.xlsx”). *S. acidocaldarius* transcriptomic data showed that 335 genes (~15% of the *S. acidocaldarius* genome) displayed a 1.5-fold ($\log_2 0.5$) or more change in expression. These included 103 genes that were up-regulated in the biofilm and 206 down-regulated genes. For *S. solfataricus*, 103 genes had an altered expression level of 1.5-fold or more (~3.4% of the *S. solfataricus* genome), the majority of which (60) were down-regulated, while 43 were up-regulated. *S. tokodaii* transcriptomic data showed that the change in expression levels was lower than those from *S. acidocaldarius* and *S. solfataricus*. Up to 32 genes were differentially regulated 1.5-fold or more in *S. tokodaii* (~1% of the genome), 15 of which that were up-regulated in biofilm and 17 of which were down-regulated.

It was determined that 51%, 59% and 66% of the differentially expressed genes corresponded to those annotated as having hypothetical or unknown function for *S. acidocaldarius*, *S. solfataricus* and *S. tokodaii*, respectively. All biofilm-regulated genes were catalogued into functional groups according to their COG category. The analysis yielded genes predominantly involved in energy production, energy conversion, amino acid metabolism, lipid and carbohydrate metabolism, transport related functions, and cell surface appendages (Figure 3). The key findings are discussed below (Table 3) and the complete data set is presented in the Supporting Information, Excel file: “Transcriptomic significant data.xlsx”.

RNA microarray experiments displayed biofilm-regulated genes encoding terminal oxidases in *Sulfolobus* spp. cells. More specifically, the data show up-regulation of the gene encoding for the polypeptide I of the cytochrome c oxidase complex *ba3* in both *S. acidocaldarius* (Saci_0097) and *S. tokodaii* (ST2595) biofilm-associated cells. In addition, a quinol oxidase-2 gene (*soxE*) was also up-regulated in *S. solfataricus* (SSO2972). In *S. acidocaldarius*, SoxE forms part of the *bb3* terminal oxidase complex SoxM (SoxEFGHIM).³⁵ In general, the findings from proteomic analyses revealed no noteworthy correlation at the transcriptomic level, and only the down-regulation of V-type ATPase subunit B encoding gene (Saci_1549) correlated on both in transcriptomic and proteomic analyses (Table 3).

As performed for the proteomic data, a BLASTp analysis was performed for each transcript using the encoded amino acid

sequences for queries of both significantly up-regulated genes and significantly down-regulated genes. By doing so, we were able to cluster biofilm-regulated genes common to all three *Sulfolobus* species (Figure 3, Table 2). From the up-regulated data set, only one gene was determined to be overexpressed in all three *Sulfolobus* species in biofilm-associated cells (Figure 2, Table 2). This change corresponds to an ATP-binding transporter (Saci_2305, SSO0053 and ST0535), most likely involved in cation detoxification. Further ORFs annotated as inorganic substrates transporters were found to be up-regulated in at least two *Sulfolobus* strains (SSO1078 and ST1577).

On the other hand, the single common biofilm down-regulated gene, or alternatively, up-regulated in planktonic cells, corresponded to a 3-oxoacyl-(acyl-carrier-protein) reductase (Saci_1792, SSO0975 and ST1299) (Table 3). Interestingly, this enzyme is involved in the production of the quorum sensing autoinducer 3-oxo-C12-HSL in *P. aeruginosa*.³⁶

Some of the genes proposed to be required for flagella biosynthesis and assembly were up-regulated in *S. acidocaldarius* biofilm-associated cells, as revealed by RNA microarrays (Table 3). The UV-inducible type IV pili related gene *upsF* (SSO0119) was up-regulated. *upsF* encodes a putative transmembrane protein proposed to form part of the membrane platform of the pili structure (Table 3).

The expression of some genes catalogued into the cell wall/membrane/envelope biogenesis functional group was also altered in *Sulfolobus* biofilm cells (Table 3). *S. acidocaldarius* displayed the overexpression of ORFs Saci_0134, which encodes a hypothetical protein sharing significant sequence similarity to an annotated NAD-dependent epimerase/dehydratase of *Metallosphaera sedula* (Msed_0434). This enzyme is potentially involved in extracellular polysaccharides (EPS) production.³⁷

DISCUSSION

General Overview

We previously described that *S. acidocaldarius*, *S. solfataricus*, and *S. tokodaii* form very different biofilm morphologies, ranging from simple carpet structures in *S. solfataricus* to high-density tower-like forming structures in *S. acidocaldarius*.¹⁰ In this study, we have further characterized the process of *Sulfolobus* biofilm formation by integrating spectroscopic analysis, transcriptomics and proteomics in order to determine how each of the three species is adapted to growth in biofilms.

As we showed through FTIR analysis, spectral data sets from biofilm cells within *Sulfolobus* biofilms differed substantially from their planktonic counterparts. In addition, we were able to show that a biofilm-associated lifestyle displayed distinct expression transcriptomic and proteomic profiles in all *Sulfolobus* species. These results resonate with those from studies of bacteria, in which proteomics and FT-IR spectroscopy with multivariate statistical analysis were combined to show a distinct, species-specific differences between the physiology of biofilm-associated and planktonic bacterial cells.^{20,21,38,39}

In addition, the expression profile as per microarray analysis showed that the biofilm lifestyle affects each strain differently. While ca. 15% of the *S. acidocaldarius* genes' expression was altered by a factor of 1.5 or more, the change in genes expression patterns represented only ~3.4 and ~1% in *S. solfataricus* and *S. tokodaii*, respectively. The percentage differences in biofilm-regulated genes between the *Sulfolobus* species are consistent with what has been reported in transcriptomes from biofilm-grown

bacteria. For example, in *E. coli*, 5.5% of ORFs were determined to have different expression patterns in biofilm-associated cells, while 14% of genes in biofilm-associated *B. subtilis* cells had a different expression pattern when compared to planktonic cells.^{40,41} Furthermore, the numbers of biofilm-regulated genes in other bacterial systems are even smaller, as *P. aeruginosa* transcriptomic experiments showed that only 1% of genes are differentially expressed in biofilms.⁴²

The difference in gene expression levels between *Sulfolobus* biofilm-associated and planktonic cells were found to be less than that of eubacteria. Thus, it is tempting to suggest that lifestyle transition from planktonic to biofilm does not radically alter the regulated transcript abundance in *Sulfolobus* biofilms. However, even slight changes in gene expression may potentially have a profound effect on cellular physiology, as has been described by analyses of transcriptomes from biofilm-associated bacteria.¹⁴

Discrepancies observed between transcriptome and proteome profiling underscores the putative role that post-transcriptional and post-translational regulation mechanisms might play in *Sulfolobus* biofilm formation. In this regard, the reduced regulation at the transcriptional level observed in *S. tokodaii* in comparison to the remarkable proteomic changes obtained suggests that the physiological effect might correspond to intense post-transcriptional regulation. Moreover, in the future we expect to gain further understanding of the role of regulatory noncoding RNAs in biofilm-associated *Sulfolobus* cells.

Energetic Adjustments during the Biofilm Mode of Life

Genes and proteins involve in energetic metabolism were highly altered in *Sulfolobus* spp. biofilm-associated population. These changes included mainly genes related to respiratory complexes, Tricarboxylic acid cycle (TCA) enzymes and V-AT-Pases subunits (Table 3, Figure 3). Genes encoding cytochrome *o* ubiquinol oxidase subunits have been also described as up-regulated in both *Salmonella enterica* serovar Tiphymurium and *E. coli* K-12 biofilm-associated cells, suggesting that the environment of these biofilms was aerobic,^{13,15} which might also be the case for *Sulfolobus* biofilms. On the other hand, previous studies have shown that terminal respiratory complexes work as proton pumps for maintaining the intracellular pH and generating proton motive force in certain *Sulfolobales*.⁴³ Moreover, it has been proposed that the SoxM complex might serve as a pH sensor and it would assume its highest activity when the pH rises to values greater than 5 in the extracellular medium.³⁵ As we previously observed, the pH in the extracellular medium during biofilm development progressively raises above 5 in *Sulfolobus* spp. cells (Koerdts et al., unpublished results). Consequently, the overexpression of Sox complex-related genes might be a response to keep the ambient pH down.

Furthermore, several genes playing a role in TCA cycle were also altered, being most of them down-regulated in biofilm-associated cells, suggesting a decreased metabolic activity in this cell population in comparison to the planktonic counterparts. V-ATPases subunits were also down-regulated in *S. acidocaldarius* biofilm-associated cells (Table 3). Conversely, the ATP synthase subunit E was found up-regulated in *S. solfataricus* biofilm-associated cells (Table 3).

Cell Surface Modifications

As we have previously described, *S. acidocaldarius* more readily engages in community formation than other *Sulfolobus* species.¹⁰ This descriptive observation is conducive with and complementary to our spectroscopic analysis. *S. acidocaldarius* showed the

most radical spectral change in comparisons of biofilm-associated versus planktonic samples. In line with this premise, XPS analysis also showed that *S. acidocaldarius* biofilm-associated cells experienced an increase of polysaccharide-containing molecules on their cell surfaces (Table 1). Interestingly, a putative glycosyl transferase-encoding gene were regulated in *S. acidocaldarius* (Table 3). Glycosyltransferases (GTs) play an important role modifying both lipid and protein components of biological membranes by the covalent addition of polysaccharides. In addition, the specific function of GTs in biosynthesis of high-molecular-weight sugar-rich heteropolymeric EPS molecules has been described in bacterial systems.⁴⁴ Moreover, GT encoding genes have been found to be overexpressed in bacterial biofilms, and their disruption alters the ability to synthesize the EPS matrix.⁴⁵ The increased expression of EPS production related genes observed in *S. acidocaldarius* biofilm cells might be correlated to its particular cell surface chemical composition. Future analyses will focus on determining their involvement in the EPS biosynthetic pathway, which is expected to involve further enzymatic activities.

Commonly Biofilm-Regulated Genes among the Three Strains

The description of biofilm-regulated genes and proteins common to all three examined *Sulfolobus* species yielded some interesting findings. All three displayed increased levels of a putative transcriptional regulator belonging to the Lrs14-like proteins (Saci_1223, SSO1101 and ST0837) (Table 2). These putative proteins are homologous to the Lrs14 protein (SSO1108) of *S. solfataricus*, the protein levels of which were also increased during the biofilm lifestyle (Table 3). It has been described that *S. solfataricus* Lrs14 (SSO1108) is autoregulated in a negative manner and accumulates in the midexponential and late growth phases.⁴⁶ Archaeal Lrs14-like regulators are thought to be related to the Lrp-AsnC bacterial transcriptional regulator family (leucine-responsive regulatory protein).⁴⁶ The Lrp *E. coli* regulon includes genes involved in amino acid biosynthesis (*ilvIH*, *serA*), in the biosynthesis of cell surface structures such as pili (*pap*, *fan*, *fim*), and in the assimilation of ammonia (*glnA*, *gltBD*).⁴⁷ However, Lrp-like regulators have not been yet directly identified as being involved in biofilms. In biofilm-associated bacteria, several global gene regulators are known to control a wide range of adaptive physiological and regulatory circuits within sessile community and to be up-regulated as a response to environmental conditions, that is, nutrient limitation, oxygen availability and osmotic stress.¹⁵ Thus, the expression of these homologous transcriptional regulators might constitute a master regulatory factor involved in *Sulfolobus* biofilm development. The functional role of Lrs14-like proteins in *Sulfolobus* biofilms is being currently investigated.

One gene, 3-oxoacyl-(acyl-carrier-protein) reductase (FabG) (Table 3), was found to be down-regulated in biofilm-associated cells (and up-regulated in planktonic cells) in all three *Sulfolobus* strains. FabG enzymatic activity is involved in the production of the Quorum Sensing (QS) autoinducer (AI) 3-oxo-dodecanoyl-HSL (3-oxo-C12-HSL) in *P. aeuruginosa*.³⁶ In bacteria, QS phenomena is known to be closely interrelated to biofilm formation. QS provides the means to coordinate the activities of cells so that they function as a multicellular community. Interestingly, FabG levels were also found to be heightened in *P. aeuruginosa* planktonic cells in comparison to their biofilm counterparts.¹⁷ Although, it seems that *Sulfolobus* genomes do not encode

LasI-homologous proteins, an utterly different mechanism employed by an unknown activity might be involved in tandem with FabG to produce putative archaeal AI molecules. In this regard, studies in biofilms of the archaeon *F. acidarmanus* Fer1 showed no evidence for quorum sensing or signaling molecules.⁸ However, the production of AI molecules by *Sulfolobus* cells still has to be proven. Furthermore, in the future, it will be of interest to determine the potential occurrence of cell signaling and communication within *Sulfolobus* biofilm-associated communities.

■ ASSOCIATED CONTENT

Supporting Information

DNA microarrays significant data of each *Sulfolobus* strains is listed in the excel file "Transcriptomic significant data.xlsx". Proteomic data analysis of each *Sulfolobus* strains is listed in the excel files: "Proteomic supplementary-1.xlsx" for *S. solfataricus* P2, "Proteomic supplementary-2.xlsx" for *S. acidocaldarius* and "Proteomic supplementary-3.xlsx" for *S. tokodaii*. Sheet 1 shows details of peptides lists and Sheet 2 shows details of quantified proteins lists. Table S1 shows binding energies, assignments and composition (%) of XPS spectral bands of *Sulfolobus acidocaldarius*, *solfataricus* and *tokodaii* grown planktonically and as biofilm. Table S2, iTRAQ labeling of samples. Table S3 shows all significant result obtained from iTRAQ proteomic analysis. Table S4, determination of gene expression by qRT-PCR. Table S5 lists qPCR oligonucleotides. This material is available free of charge via the Internet at <http://pubs.acs.org>.

■ AUTHOR INFORMATION

Corresponding Author

*S.-V. Albers, e-mail: albers@mpi-marburg.mpg.de. Tel.: +496421178426. Fax: +496421178429.

Author Contributions

†These authors contributed equally to this manuscript

■ ACKNOWLEDGMENT

A.K., A.O. and S.-V.A. were supported by intramural funds of the Max Planck Society. S.-V.A. received additional support by a VIDI grant from the Dutch Science Organization (NWO). EPSRC (S&I Grant EP/E036252/1), BBSRC (under the SysMO Programme – SulfoSys; BBF0034201)

■ REFERENCES

- (1) Lopez, D.; Vlamakis, H.; Kolter, R. Biofilms. *Cold Spring Harb. Perspect. Biol.* **2010**, *2* (7), a000398.
- (2) Kruger, M.; Blumenberg, M.; Kasten, S.; Wieland, A.; Kanel, L.; Klock, J. H.; Michaelis, W.; Seifert, R. A novel, multi-layered methanotrophic microbial mat system growing on the sediment of the Black Sea. *Environ. Microbiol.* **2008**, *10* (8), 1934–47.
- (3) Zhang, C. L.; Ye, Q.; Huang, Z.; Li, W.; Chen, J.; Song, Z.; Zhao, W.; Bagwell, C.; Inskip, W. P.; Ross, C.; Gao, L.; Wiegel, J.; Romanek, C. S.; Shock, E. L.; Hedlund, B. P. Global occurrence of archaeal amoA genes in terrestrial hot springs. *Appl. Environ. Microbiol.* **2008**, *74* (20), 6417–26.
- (4) Rinker, K. D.; Kelly, R. M. Growth Physiology of the Hyperthermophilic Archaeon *Thermococcus litoralis*: Development of a Sulfur-Free Defined Medium, Characterization of an Exopolysaccharide, and Evidence of Biofilm Formation. *Appl. Environ. Microbiol.* **1996**, *62* (12), 4478–85.

- (5) Näther, D. J.; Rachel, R.; Wanner, G.; Wirth, R. Flagella of *Pyrococcus furiosus*: multifunctional organelles, made for swimming, adhesion to various surfaces, and cell-cell contacts. *J. Bacteriol.* **2006**, *188* (19), 6915–6923.
- (6) Schopf, S.; Wanner, G.; Rachel, R.; Wirth, R. An archaeal bi-species biofilm formed by *Pyrococcus furiosus* and *Methanopyrus kandleri*. *Arch. Microbiol.* **2008**, *190* (3), 371–7.
- (7) Lapaglia, C.; Hartzell, P. L. Stress-Induced Production of Biofilm in the Hyperthermophile *Archaeoglobus fulgidus*. *Appl. Environ. Microbiol.* **1997**, *63* (8), 3158–63.
- (8) Baker-Austin, C.; Potrykus, J.; Wexler, M.; Bond, P. L.; Dopson, M. Biofilm development in the extremely acidophilic archaeon 'Ferropasma acidarmanus' Fer1. *Extremophiles* **2010**, *14* (6), 485–491.
- (9) Zolghadr, B.; Klingl, A.; Koerdt, A.; Driessen, A. J.; Rachel, R.; Albers, S. V. Appendage-mediated surface adherence of *Sulfolobus solfataricus*. *J. Bacteriol.* **2010**, *192* (1), 104–10.
- (10) Koerdt, A.; Gödeke, J.; Berger, J.; Thormann, K. M.; Albers, S. V. Crenarchaeal biofilm formation under extreme conditions. *PLoS One* **2010**, *5* (11), e14104.
- (11) Sauer, K. The genomics and proteomics of biofilm formation. *Genome Biol.* **2003**, *4* (6), 219.
- (12) Beloin, C.; Valle, J.; Latour-Lambert, P.; Faure, P.; Kzreminski, M.; Balestrino, D.; Haagensen, J. A.; Molin, S.; Prensier, G.; Arbeille, B.; Ghigo, J. M. Global impact of mature biofilm lifestyle on *Escherichia coli* K-12 gene expression. *Mol. Microbiol.* **2004**, *51* (3), 659–74.
- (13) Beloin, C.; Ghigo, J. M. Finding gene-expression patterns in bacterial biofilms. *Trends Microbiol.* **2005**, *13* (1), 16–9.
- (14) Schembri, M. A.; Kjaergaard, K.; Klemm, P. Global gene expression in *Escherichia coli* biofilms. *Mol. Microbiol.* **2003**, *48* (1), 253–67.
- (15) Hamilton, S.; Bongaerts, R. J. M.; Mulholland, F.; Cochrane, B.; Porter, J.; Lucchini, S.; Lappin-Scott, H. M.; Hinton, J. C. D. The transcriptional programme of *Salmonella enterica* serovar Typhimurium reveals a key role for tryptophan metabolism in biofilms. *BMC Genomics* **2009**, *10*, 599–620.
- (16) Wen, Z. T.; Burne, R. A. Functional genomics approach to identifying genes required for biofilm development by *Streptococcus mutans*. *Appl. Environ. Microbiol.* **2002**, *68* (3), 1196–203.
- (17) Nigaud, Y.; Cosette, P.; Collet, A.; Song, P. C.; Vaudry, D.; Vaudry, H.; Junter, G. A.; Jouenne, T. Biofilm-induced modifications in the proteome of *Pseudomonas aeruginosa* planktonic cells. *Biochim. Biophys. Acta* **2010**, *1804* (4), 957–66.
- (18) Oosthuizen, M. C.; Steyn, B.; Lindsay, D.; Brozel, V. S.; von Holy, A. Novel method for the proteomic investigation of a dairy-associated *Bacillus cereus* biofilm. *FEMS Microbiol. Lett.* **2001**, *194* (1), 47–51.
- (19) Steyn, B.; Oosthuizen, M. C.; MacDonald, R.; Theron, J.; Brozel, V. S. The use of glass wool as an attachment surface for studying phenotypic changes in *Pseudomonas aeruginosa* biofilms by two-dimensional gel electrophoresis. *Proteomics* **2001**, *1* (7), 871–9.
- (20) Mukherjee, J.; Ow, S. Y.; Noirel, J.; Biggs, C. A. Quantitative protein expression and cell surface characteristics of *Escherichia coli* MG1655 biofilm. *Proteomics* **2010**, *11* (3), 339–351.
- (21) Serra, D. O.; Lücking, G.; Weiland, F.; Schulz, S.; Görg, A.; Yantorno, O. M.; Ehling-Schulz, M. Proteome approaches combined with Fourier transform infrared spectroscopy revealed a distinctive biofilm physiology in *Bordetella pertussis*. *Proteomics* **2008**, *8* (23–24), 4995–5010.
- (22) Naumann, D., *Infrared spectroscopy in microbiology. Encyclopedia of analytical chemistry*; John Wiley and Sons Ltd.: Chichester, 2000.
- (23) Ojeda, J. J.; Romero-Gonzalez, M. E.; Bachmann, R. T.; Edyvean, R. G.; Banwart, S. A. Characterization of the cell surface and cell wall chemistry of drinking water bacteria by combining XPS, FTIR spectroscopy, modeling, and potentiometric titrations. *Langmuir* **2008**, *24* (8), 4032–40.
- (24) Zaparty, M.; Esser, D.; Gertig, S.; Haferkamp, P.; Kouril, T.; Manica, A.; Pham, T. K.; Reimann, J.; Schreiber, K.; Sierocinski, P.; Teichmann, D.; van Wolferen, M.; von Jan, M.; Wieloch, P.; Albers, S. V.; Driessen, A. J.; Klenk, H. P.; Schleper, C.; Schomburg, D.; van der Oost, J.; Wright, P. C.; Siebers, B. "Hot standards" for the thermoacidophilic archaeon *Sulfolobus solfataricus*. *Extremophiles* **2009**, *14* (1), 119–42.
- (25) Pham, T. K.; Roy, S.; Noirel, J.; Douglas, I.; Wright, P. C.; Stafford, G. P. A quantitative proteomic analysis of biofilm adaptation by the periodontal pathogen *Tannerella forsythia*. *Proteomics* **2010**, *10* (17), 3130–41.
- (26) Eboigbodin, K. E.; Biggs, C. A. Characterization of the extracellular polymeric substances produced by *Escherichia coli* using infrared spectroscopic, proteomic, and aggregation studies. *Biomacromolecules* **2008**, *9* (2), 686–95.
- (27) Piatek, R.; Bruździak, P.; Zalewska-Piatek, B.; Kur, J.; Stangret, J. Preclusion of irreversible destruction of Dr adhesin structures by a high activation barrier for the unfolding stage of the fimbrial DraE subunit. *Biochemistry* **2009**, *48* (49), 11807–16.
- (28) Helm, D.; Labischinski, H.; Schallehn, G.; Naumann, D. Classification and identification of bacteria by Fourier-transform infrared spectroscopy. *J. Gen. Microbiol.* **1991**, *137* (1), 69–79.
- (29) Jiang, W.; Saxena, A.; Song, B.; Ward, B. B.; Beveridge, T. J.; Myneni, S. C. Elucidation of functional groups on gram-positive and gram-negative bacterial surfaces using infrared spectroscopy. *Langmuir* **2004**, *20* (26), 11433–42.
- (30) Geoghegan, M.; Andrews, J. S.; Biggs, C. A.; Eboigbodin, K. E.; Elliott, D. R.; Rolfe, S.; Scholes, J.; Ojeda, J. J.; Romero-Gonzalez, M. E.; Edyvean, R. G.; Swanson, L.; Rutkaite, R.; Fernando, R.; Pen, Y.; Zhang, Z.; Banwart, S. A. The polymer physics and chemistry of microbial cell attachment and adhesion. *Faraday Discuss.* **2008**, *139*, 85–103. discussion105–28. 419–20.
- (31) Serra, D. O.; Lücking, G.; Weiland, F.; Schulz, S.; Gorg, A.; Yantorno, O. M.; Ehling-Schulz, M. Proteome approaches combined with Fourier transform infrared spectroscopy revealed a distinctive biofilm physiology in *Bordetella pertussis*. *Proteomics* **2008**, *8* (23–24), 4995–5010.
- (32) Bosch, A.; Serra, D.; Prieto, C.; Schmitt, J.; Naumann, D.; Yantorno, O. Characterization of *Bordetella pertussis* growing as biofilm by chemical analysis and FT-IR spectroscopy. *Appl. Microbiol. Biotechnol.* **2006**, *71* (5), 736–47.
- (33) Clarke, D. J.; Ortega, X. P.; Mackay, C. L.; Valvano, M. A.; Govan, J. R.; Campopiano, D. J.; Langridge-Smith, P.; Brown, A. R. Subdivision of the bacterioferritin comigratory protein family of bacterial peroxiredoxins based on catalytic activity. *Biochemistry* **2010**, *49* (6), 1319–30.
- (34) Guagliardi, A.; Napoli, A.; Rossi, M.; Ciaramella, M. Annealing of complementary DNA strands above the melting point of the duplex promoted by an archaeal protein. *J. Mol. Biol.* **1997**, *267* (4), 841–8.
- (35) Komorowski, L.; Verheyen, W.; Schafer, G. The archaeal respiratory supercomplex SoxM from *S. acidocaldarius* combines features of quinole and cytochrome c oxidases. *Biol. Chem.* **2002**, *383* (11), 1791–9.
- (36) Hoang, T. T.; Sullivan, S. A.; Cusick, J. K.; Schweizer, H. P. Beta-ketoacyl acyl carrier protein reductase (FabG) activity of the fatty acid biosynthetic pathway is a determining factor of 3-oxo-homoserine lactone acyl chain lengths. *Microbiology* **2002**, *148* (Pt 12), 3849–56.
- (37) Auernik, K. S.; Maezato, Y.; Blum, P. H.; Kelly, R. M. The genome sequence of the metal-mobilizing, extremely thermoacidophilic archaeon *Metallosphaera sedula* provides insights into bioleaching-associated metalolism. *Appl. Environ. Microbiol.* **2008**, *74* (3), 682–92.
- (38) Vilain, S.; Brozel, V. S. Multivariate approach to comparing whole-cell proteomes of *Bacillus cereus* indicates a biofilm-specific proteome. *J. Proteome Res.* **2006**, *5* (8), 1924–30.
- (39) Vilain, S.; Cosette, P.; Hubert, M.; Lange, C.; Junter, G. A.; Jouenne, T. Comparative proteomic analysis of planktonic and immobilized *Pseudomonas aeruginosa* cells: a multivariate statistical approach. *Anal. Biochem.* **2004**, *329* (1), 120–30.
- (40) Ren, D.; Bedzyk, L. A.; Setlow, P.; Thomas, S. M.; Ye, R. W.; Wood, T. K. Gene expression in *Bacillus subtilis* surface biofilms with and without sporulation and the importance of yveR for biofilm maintenance. *Biotechnol. Bioeng.* **2004**, *86* (3), 344–64.

(41) Ren, D.; Bedzyk, L. A.; Thomas, S. M.; Ye, R. W.; Wood, T. K. Gene expression in *Escherichia coli* biofilms. *Appl. Microbiol. Biotechnol.* **2004**, *64* (4), 515–24.

(42) Whiteley, M.; Banger, M. G.; Bumgarner, R. E.; Parsek, M. R.; Teitzel, G. M.; Lory, S.; Greenberg, E. P. Gene expression in *Pseudomonas aeruginosa* biofilms. *Nature* **2001**, *413* (6858), 860–4.

(43) Lubben, M.; Arnaud, S.; Castresana, J.; Warne, A.; Albracht, S. P.; Saraste, M. A second terminal oxidase in *Sulfolobus acidocaldarius*. *Eur. J. Biochem.* **1994**, *224* (1), 151–9.

(44) Lebeer, S.; Verhoeven, T. L.; Francius, G.; Schoofs, G.; Lambrechts, I.; Dufrene, Y.; Vanderleyden, J.; De Keersmaecker, S. C. Identification of a Gene Cluster for the Biosynthesis of a Long, Galactose-Rich Exopolysaccharide in *Lactobacillus rhamnosus* GG and Functional Analysis of the Priming Glycosyltransferase. *Appl. Environ. Microbiol.* **2009**, *75* (11), 3554–63.

(45) Koo, H.; Xiao, J.; Klein, M. I.; Jeon, J. G. Exopolysaccharides produced by *Streptococcus mutans* glucosyltransferases modulate the establishment of microcolonies within multispecies biofilms. *J. Bacteriol.* **2010**, *192* (12), 3024–32.

(46) Napoli, A.; van der Oost, J.; Sensen, C. W.; Charlebois, R. L.; Rossi, M.; Ciaramella, M. An Lrp-like protein of the hyperthermophilic archaeon *Sulfolobus solfataricus* which binds to its own promoter. *J. Bacteriol.* **1999**, *181* (5), 1474–80.

(47) Calvo, J. M.; Matthews, R. G. The leucine-responsive regulatory protein, a global regulator of metabolism in *Escherichia coli*. *Microbiol. Rev.* **1994**, *58* (3), 466–90.